Separation and purification of amygdalin from thinned bayberry kernels by macroporous adsorption resins

Running title: Separation of bayberry amygdalin

Tao Wang[a,b], Shengmin Lu[a*], Qile Xia[a], Zhongxiang Fang[c], Stuart Johnson [c]

[a] *Key Laboratory of Fruits and Vegetables Postharvest and Processing of Zhejiang Province, Institute of Food Science, Zhejiang Academy of Agricultural Science, Hangzhou 310021, PR China*

[b] *Zhejiang Normal University, Jinhua 321000, PR China*

[c] *Food Science & Technology Program, School of Public Health, Faculty of Health Sciences, International Institute of Agri-Food Security (IIAFS), Curtin University, GPO Box U1987, Perth, 6845, WA, Australia*

[*] Corresponding author at: Key Laboratory of Fruits and Vegetables Postharvest and Processing of Zhejiang Province, Institute of Food Science, Zhejiang Academy of Agricultural Science, Hangzhou 310021, PR China. Tel.: +86 571 86417306.

E-mail address: lushengmin@hotmail.com (S. Lu)

ABSTRACT

To utilize the low-value thinned bayberry (*Myrica rubra* Sieb. et Zucc) kernels (TBKs) waste, an efficient method using macroporous adsorption resins (MARs) for separation and purification of amygdalin from TBKs crude extracts was developed. An aqueous crude sample was prepared from a methanol TBK extract, followed by resin separation. A series of MARs were initially screened for adsorption/desorption of amygdalin in the extract, and D101 was selected for characterization and method development. The static adsorption data of amygdalin on D101 was best fitted to the pseudo-second-order kinetics model. The solute affinity towards D101 at 30 °C was described and the equilibrium experimental data were well-fitted to Langmuir and Freundlich isotherms. Through one cycle of dynamic adsorption/desorption, the purity of amygdalin in the extract, determined by HPLC, increased about 17-fold from 4.8% to 82.0%, with 77.9% recovery. The results suggested that D101 resin effectively separate amygdalin from TBKs.

Keywords: Bayberry; A*mygdalin; Tthinned bayberry kernels (TBKs); Macroporous adsorption resins (MARs); Purification*

1. Introduction

Bayberry (*Myrica rubra* Sieb. et Zucc.) is a fruit tree native to China, mainly south of Yangtze river, and typically in Zhejiang province. The bayberry tree has a high fruit-setting rate and manual thinning (removal of young, immature fruits during the growing season) is commonly practiced to achieve a higher productivity and improve quality of the remaining fruit [1]. The thinned fruits are usually regarded as waste and discarded. Compared with the mature bayberry fruit, thinned fruit has a higher proportion of stones in a range of 19.6-34.2% (g/100 g fresh weight [FW]). Each fruit stone contains one kernel and these kernels from mature fruit stone are reported to be rich in nutrients such as crude fiber, fat, vitamins, proteins and minerals [2]. The kernels may be crushed and used as nutritious supplements for animal feed and also have potential for development into high value-added products such as polyphenols, vegetable fats and vegetable protein [3]. Preliminary investigations on TBKs reported average contents of moisture, protein, fats and carbohydrates of 30.2%, 28.0%, 58.4% and 1.8% respectively. In addition to valuable nutritional components, bayberry kernels have also been reported to contain amygdalin, a cyanogenic glycoside with potential pharmacological and toxicological effects [2].

Amygdalin is found in seeds and leaves of loquat, apricot, peach, plum and other *Rosaceae* species. Amygdalin is an α-hydroxy benzyl nitrile, consisting of the aglycone mandelonitrile, and the disaccharide gentiobiose (6-o-β-d-glucopyranosyl-d-glucose) (Fig.1), with a formula of $C_{20}H_{27}O_{11}N$ and

molecular weight of 458 [4]. It was reported that amygdalin may play a role in relieving cough and asthma in humans [5]; regulate immune function and demonstrate anti-tumor activity [6]. Cyanogenic glycosides have high toxicity potential upon ingestion, however the toxicity potential for amygdalin was reported as very low [7]. Amygdalin from loquat seeds has been proved to be therapeutically potential in preventing and / or treating of atherosclerosis, gastric ulcer, psoriasis, arthritis and wound healing [8-12]. However there is little reported research on amygdalin from TBKs, and its phytochemical properties and possible medicinal uses are not fully investigated.

Macroporous adsorption resins (MARs) are efficient matrices for enrichment of bioactive substances from plant resources due to their high selectivity and adsorption capacity, as well as stability and resistance to degradation by osmotic shock and oxidation [13]. They are a group of polymers containing a permanent network of pores independent of the state of swelling of the resin and thus display much better solvent tolerance than gel-type resins. The adsorption performance of MARs is closely related to its polarity. Non-polar resins with strong hydrophobic pore surface, without any functional groups, are suitable for adsorbing non-polar substances; medium-polar resins with both hydrophilic and hydrophobic surface properties, containing an ester group, are suitable for adsorbing both non-polar and polar substances; and polar resins adsorb polar substance mainly through electrostatic interactions [14-15]. The isolation of plant polyphenolic compounds routinely use MARs such as Amberlite XAD resin or Sephadex [16-18]. Although solid-phase

extraction and purification (e.g. C_{18} Sep-Pak cartridge) are commonly used before HPLC determination of bioactive compounds [19], MARs are more efficient in enrichment of bioactive compounds if its concentration in plant is relatively low [13]. To our knowledge, there is no published report using MARs for purification of cyanogenic glycosides.

An efficient method for the purification of amygdalin from TBKs might provide value-addition opportunities for the utilization of this low-value thinned fruit waste. Therefore the aim of this study was to determine the static and dynamic adsorption/desorption parameters of amygdalin from TBKs extract using macroporous resin chromatography.

2. Materials and methods

2.1. Chemicals, reagents and samples

Ethanol of analytical grade was purchased from East Pharmaceutical Technology Co., Ltd. (Hangzhou, China); Acetonitrile of HPLC grade, and amygdalin were purchased from J&K Scientific Ltd. (Beijing, China). Distilled water was used throughout. The cultivar of thinned bayberry fruits was Ding-ao which was collected from Wenzhou city (Zhejiang Province, China) in June, 2012. When the thinned bayberry was arrived at our laboratory, stones were separated by removing the outer villiform pulp after lyophilizing the whole fruits. The stones were broken by cracking

with a micro-punch to obtain the kernels (5.68±0.33 g of weight/100 kernels in average), and the kernels were sealed in aluminum foil bags and stored at -40°C for subsequent analysis.

MARs of HPD722, HPD720, AB-8, NKA-9, D101, HPD100 and HPD400 were purchased from Cangzhou Bon Adsorber Technology Co., Ltd. (Hebei Province, China). These are the most commonly used resins in separation of plant bioactive substance in China [20-21]. Specifications of the MARs are shown in Table 1. The resins were soaked in 95% ethanol for 24 h and then washed by distilled water before use.

2.2. HPLC analysis of amygdalin

The HPLC system (Dalian Elite Instrument Co., Ltd., China) consisted of a P230 pump equipped with a 230^{+} diode array detector set at 214 nm. A Symmetry® C18 MG column (4.6 mm×250 mm, 5 μm, Waters Ltd., Ireland) was maintained at 25°C. The mobile phase was 13% acetonitrile in water at a flow rate of 1.0 ml/min. Standard solutions of amygdalin with the concentrations of 0, 100, 200, 300, 400 mg l^{-1} were filtered through 0.45 μm membrane filters and each of 10 μl was injected into the HPLC system to get the standard curve. The concentration of amygdalin both in crude and purified extracts was determined as follows [22]: 0.25 g extract was dissolved in 25 ml methanol solution, treated in ultrasound (250 W, 50 kHz) for 30 min; and then filtered through a Whatman No. 1 filter paper using a Buchner funnel. A 1 ml extract

124 solution was diluted 50x with 50% methanol (aq.) and injected into the HPLC system
125 and its concentration was determined from the calibration curve.
126
127 *2.3. Preparation of sample solutions of amygdalin crude extract*
128
129 The bayberry kernels were dried at 105°C for enzyme inactivation and defatted
130 with 20 volumes petroleum ether (boiling at 60-90°C for 2 h) for three times. Then the
131 kernels were ground into powder and passed through a 60 mesh sieve. Bayberry
132 kernel powder was extracted with 20 volumes methanol solution in a flask (45°C for
133 30 min), and repeated three times. The extract solutions were combined and vacuum
134 filtered through a Whatman No. 1 filter paper using a Buchner funnel. The filtrate was
135 evaporated in a rotary evaporator (RE 52-99, Shanghai Yarong Biochemical
136 Instrument Factory, China) under reduced pressure at 45°C to remove the methanol.
137 The residue was diluted with distilled water to give the crude TBK solution before
138 being loaded onto the chromatography column.
139
140 *2.4. Static adsorption/desorption experiments*
141
142 *2.4.1. Adsorption resin screening*
143 The amygdalin static adsorption experiments using different resins were carried
144 out as follows: 0.5 g resin was added into 50 ml crude TBK solution with an
145 amygdalin concentration of 380.76 mg l^{-1} (determined by HPLC) in a 250 ml conical

flask. The flask was continually shaken in a HZ-9511K incubator (100 rpm) (Hua Lida Experimental Equipment Co., Ltd., Jiangsu province, China) at 30 °C for 24 h. After the adsorption equilibrium, the sample was filtered through a 0.45 μm membrane filter and analyzed by HPLC as in section 2.2. The static desorption experiments were carried out as follows: 60 ml ethanol (aq.) at a concentration of 50% (*v/v*) was added to the adsorbate-laden resins separated from the adsorption solution in the 250 ml conical flask. The flask was continually shaken in the incubator (100 rpm) at 30°C for 24 h. After filtration through a Whatman No. 1 filter paper using a Buchner funnel, the concentration of amygdalin in desorption solution was analyzed by HPLC. The optimum resin of MARs was determined by their efficiency and capacities of adsorption/desorption, and the calculation equations were as follows:

Adsorption efficiency:

$$A(\%) = \frac{C_0 - C_e}{C_0} \times 100\% \quad (1)$$

Adsorption capacity:

$$q_e = \frac{V_0 \times (C_0 - C_e)}{W \times (1 - M)} \quad (2)$$

Desorption efficiency:

$$D(\%) = \frac{C_d \times V_d}{(C_0 - C_e) \times V_0} \times 100\% \quad (3)$$

Where, A is the adsorption efficiency (%), q_e is the adsorption capacity (mg g^{-1} dry resin) at adsorption equilibrium, and D is the desorption efficiency (%). C_0 and C_e are the initial and equilibrium concentrations of amygdalin solutions, respectively (mg l^{-1}), and C_d is the amygdalin concentration in the desorption solution (mg l^{-1}). W is the

weight of the resin (g); M is the moisture content of resin (%). V_0 and V_d are the volume of amygdalin solution and ethanol (aq.) respectively (ml).

2.4.2. Adsorption kinetics

Static adsorption kinetics curves describe the change of adsorption amount over time. The adsorption kinetics curve of amygdalin on the selected resin was studied as following process: 0.5 g selected resin was added into 50 ml amygdalin solution (114.71 mg l^{-1}) in a 250 ml conical flask. The flask was continually shaken (100 rpm) in an incubator at 30 °C for 24 h. Liquid sample of 0.5 ml was pipetted at time intervals of 5, 10, 15, 30, 60, 120 and 180 min, and the concentration of amygdalin was determined by HPLC. Triplicates were performed for this analysis.

To better understand the adsorption mechanism, the pseudo-first-order, pseudo-second-order and intra-particle diffusion kinetic model were used to evaluate the adsorption kinetics of amygdalin to the selected resins. These models are commonly used in adsorption kinetics study and the model equations are as follows [23].

Pseudo-first-order model:

$$\log(q_e - q_t) = -\frac{k_1}{2.303} t + \log q_e \quad (4)$$

Pseudo-second-order model:

$$\frac{t}{q_t} = \frac{1}{q_e} t + \frac{1}{k_2 q_e^2} \quad (5)$$

Intra-particle diffusion kinetic model:

$$q_t = k_{id} t^{1/2} + C \quad (6)$$

Where, q_e and q_t (mg g^{-1}) are the adsorption capacity at equilibrium and at time t; k_1 (min^{-1}), k_2 (g/mg/min) and k_{id} (mg/g/$min^{1/2}$) are the rate constants of pseudo-first-order model, pseudo-second-order model and intra-particle diffusion kinetic model, respectively; and C (mg g^{-1}) is a constant, representing boundary layer thickness.

2.4.3. Adsorption isotherm

Adsorption isotherms describe the equilibrium distribution of a solute between the adsorbent and the liquid phase. In practice, Langmuir model and Freundlich model are considered to be the most popular models for adsorption process [24]. The Langmuir model assumes monomolecular layer adsorption with a homogeneous distribution of adsorption energies and without mutual interaction between adsorbed molecules [25]. The Freundlich model is a two-parameter model for liquid and gas phase adsorption [26].

Six crude TBK solutions with different initial amygdalin concentrations (26.05, 77.75, 129.13, 275.04, 358.68 and 728.35 mg l^{-1}) were employed to investigate the effect of amygdalin concentration on the adsorption process. The selected resin (0.5 g) was added to each crude TBK solution (50 ml) and shaken (100 rpm) for 24 h at 30 °C. The initial and equilibrium concentrations of amygdalin were determined by HPLC to obtain the adsorption isotherm of amygdalin on the resin. The Langmuir and Freundlich models were used to interpret the adsorption experimental data, and the theoretical model parameters values were obtained from the linearized equations at

30 °C. The equations are as follows:

Langmuir model:

$$q_e = \frac{q_m C_e}{K_L + C_e} \quad (7)$$

Freundlich model:

$$q_e = K_F C_e^{\frac{1}{n}} \quad (8)$$

where, q_m (mg g^{-1}) is the maximum adsorption capacity to form monolayer on the resin. K_L is the parameter relative to the adsorption energy. K_F and n reflect the adsorption capacity and adsorption intensity of the resin respectively. q_e (mg g^{-1}) and C_e (mg l^{-1}) are the same in equation (2).

2.4.4. Optimization of the eluent concentration

After the adsorption equilibrium, the resin was filtered and washed with pure water. Afterwards, 0.5 g adsorbate-laden resin and 60 ml ethanol eluent at different concentrations in a range of 20-90% (*v/v*) were added into each of the 250 ml conical flasks and shaken (100 rpm) for 24 h at 30°C. The amygdalin concentrations in desorption solutions were determined by HPLC. Desorption efficiency of amygdalin to each elute concentration was obtained by calculation as in equation (3).

2.5. Dynamic adsorption/desorption experiments

Dynamic adsorption/desorption experiments were carried out in a glass column (2.5×30 cm) packed with the selected resin (~24 g in dry weight). The bed volume

233 (BV) and the length of the wet-packed resin were 60 ml and 23 cm, respectively. The
234 adsorption/desorption process was performed as follows: 64 ml crude TBK solution
235 with the concentration of 302.72 mg l^{-1} was loaded onto the column, and the column
236 was firstly washed with distilled water, and subsequently with ethanol solution. The
237 fraction collector was used for collecting the eluent solution. About 8 ml eluent was
238 collected in each tube and every five tubes were combined to determine the
239 concentration of amygdalin by HPLC. The change of amygdalin concentration with
240 eluent volume was plotted to get the dynamic desorption curve. In addition, the eluent
241 solutions were further concentrated and dried under vacuum to calculate the purity of
242 the product.

243 The crude TBK solution was loaded onto the macroporous resin column at
244 different flow rate (1, 2, 3 BV/h) to select the most suitable loading flow rate. The
245 loading volume experiment was performed as follows: 200 ml crude TBK solution
246 with the initial concentration of 207.25 mg l^{-1} was loaded onto the chromatography
247 column, then the effluent solution was collected and its amygdalin concentration was
248 monitored. The change of amygdalin concentration in the effluent with the loading
249 volume was plotted to get the dynamic leakage curve and the leakage point. The
250 leakage point was defined at which effluent solution concentration reached 10% of the
251 initial concentration of loading solution [27].

252

253 2.6. *Statistical analysis*

254

One-way analysis of variance (ANOVA) (SPSS 10.0 statistics software, SPSS Inc., Chicago, IL) was used for the determination of differences from triplicates determinations. The results were expressed as means ± standard deviations and considered significantly different when $P < 0.05$.

3. Results and discussion

3.1. Standard curve of amygdalin and the concentration in the crude extract

According to the method in section 2.2, a very good regression equation for HPLC determination of amygdalin ($y = 4.7657x+8.562$, $R^2 = 0.9997$) was obtained, where y was the peak area of amygdalin and x was the amygdalin concentration (mg l^{-1}). The HPLC chromatograms of the crude TBK sample and authentic amygdalin standard are shown in Fig.2. The purity of amygdalin in the crude TBK sample was determined to be 4.83% (w/w).

3.2. Screening of optimum resin

Adsorption/desorption properties of seven MARs from the static adsorption/desorption tests are shown in Fig. 3(A). For adsorption efficiency, resins of HPD722, HPD720, AB-8, NKA-9, and D101 were higher than the other two resins of HPD100, HPD400. However, for desorption efficiency, HPD720, AB-8 and D101

277 resins were significantly higher than those of other resins. Thus, HPD720, AB-8 and
278 D101 were selected for further screening. Crude TBK solutions with different
279 concentrations were mixed with one of the three kinds of resins, the next steps were
280 done as in section 2.4.1, and then the adsorption capacity and desorption efficiency
281 were obtained, as shown in Fig. 3(B). Resins of D101 and AB-8 showed similar
282 adsorption capacity and were higher than that of HPD720 resin. However, the
283 desorption efficiency of D101 was considerably higher than those of the other two
284 resins.

285 It was suggested that the performance of MARs is related to its physical and
286 chemical properties, and the efficiency of a chromatographic process is mainly
287 dependent on the adsorbent, the structure and polarity of resins [28]. Through small
288 dipole moment, non-polar macroporous resins are polymerized by monomers which
289 have strong hydrophobicity on pore surface albeit without any functional groups.
290 Therefore, non-polar macroporous resins could effectively interact with the
291 hydrophobic moiety of amygdalin. In the present study, D101 resin showed an
292 outstanding adsorption/desorption properties with amygdalin due to its excellent
293 non-polarity (Table 1). Considering the adsorption/desorption efficiency and
294 adsorption capacity, D101 was selected as the resin for isolating of amygdalin in the
295 TBK sample in further investigations.

296

297 *3.3. Adsorption kinetics of amygdalin on D101 resin*

298

299 The static adsorption kinetic curve of amygdalin on D101 resin is shown in
300 Fig.3(C). The adsorption rate of D101 for amygdalin rapidly increased in the first 25
301 min, and thereafter increased slowly. The adsorption reached equilibrium at about 45
302 min. The rapid adsorption process of D101 in the first 25 min was probably a result of
303 the high diffusivity of amygdalin into the porous structure of the resin. The adsorption
304 rate decreased as amygdalin concentration decreased as well as when the resin
305 binding surface is approaching saturation.

306 After model fitting, the linear regression correlation coefficients of the
307 pseudo-first-order equation, pseudo-second-order equation and intra-particle diffusion
308 kinetic equation were 0.5974, 0.9999 and 0.4724, respectively. Thus the
309 pseudo-second-order was considered to be the most suitable model for describing the
310 whole adsorption process. The principle of pseudo-second-order kinetics implied that
311 concentrations of both adsorbate and adsorbent were involved in rate determining step
312 in the adsorption process, which may be chemical adsorption or chemisorptions [23,
313 29]. Although the plot for the intra-particle diffusion kinetic model (R^2=0.4724)
314 showed low representation of the whole adsorption process, it could explain the
315 mechanism of adsorption in particular stages. In the present study, the adsorption
316 process of amygdalin included the boundary layer diffusion stage (0-5 min), the
317 gradual adsorption stage (5-25 min) which was intra-particle diffusion rate-limited,
318 and the equilibrium stage (25-45 min) (Fig. 3(C)). These stages were also observed in
319 separation of phenolics and rosmarinic acid from *Rabdosia serra* using macroporous
320 resins [30]. Therefore, multiple rate-controlled steps had mutual effects on the

adsorption process of amygdalin on resin D101.

3.4. Adsorption isotherm of amygdalin on D101

To further investigate the adsorption behavior of amygdalin on D101 resin, the equilibrium adsorption isotherm was constructed at the temperature of 30 °C. The initial amygdalin concentration of crude TBK solution was 26.05, 77.75, 129.13, 275.04, 358.68 and 728.35 mg l^{-1}, respectively. As shown in Fig. 3(D), the equilibrium adsorption isotherm of amygdalin on D101 resin tended to be a straight line which suggested that the adsorption process occurred in a very dilute solution [24]. The adsorption rate of D101 increased with the amygdalin concentration of crude TBK solution, considerable in the range of 129.13-358.68 mg l^{-1}, and reached a saturation plateau when the amygdalin concentration was 358.68 mg l^{-1}. Thus, the amygdalin concentration of crude TBK solution for adsorption was selected between the ranges of 129-358 mg l^{-1}.

The Langmuir Eq. (7) was converted to the linearized form with C_e and C_e/q_e as independent variable, and the Freundlich Eq. (8) was converted to the power form with C_e and q_e as independent variable. The experimental data were statistically analyzed, and the parameters K_L, K_F and n was obtained simultaneously. As shown in Table 2, the correlation coefficients of both Langmuir and Freundlich equations for amygdalin were rather high, and this indicated the adsorption process was a monomolecular layer adsorption with a homogenous distribution among the

adsorption sites at different energies [20]. In most cases, when the parameter *n* in the Freundlich model is between 1 and 10, the resin shows beneficial adsorption [31]. In the present study the n value was 1.1062, which indicated that D101 resin is appropriate for the separation of amygdalin.

3.5. Optimization of the eluent concentration

Since amygdalin is mainly used as a pharmaceutical ingredient, aqueous ethanol which is low in toxicity, was selected as the eluent. First, the eluent rate was selected as 1, 2 and 3 BV/h, and the desorption efficiency was 82.66, 80.88 and 76.99%, respectively. With the view to shorter working time and lower volume consumption, the desorption flow rate was set as 2 BV/h.

As shown in Fig. 3(E), the concentration of ethanol (aq.) had a significant impact ($P<0.05$) on the desorption efficiency of amygdalin. When the ethanol concentration was 20% and 30%, the desorption efficiency were rather low (16.33 and 22.14% respectively). With the ethanol concentration increased, the desorption efficiency was significantly increased, and reached the maximum of 80.79% at 40% ethanol (aq.) (*v/v*). The proposed mechanism of the elution process was that the eluent (ethanol aq.) outcompeted the adsorbate for adsorption onto the macroporous resin and this led to partial dissolution of the adsorbate into eluent [32]. In the present study, as the proportion of ethanol increased, the competitiveness of which was enhanced and the dissolution rate of amygdalin also improved. As the ethanol concentration increased

365 further, the desorption efficiency decreased, possibly due to increasing concentration
366 of alcohol-soluble impurities in the eluent and resulting in the decreasing of
367 amygdalin concentration. Thus, the optimal eluent for desorption of amygdalin from
368 D101 resin was 40% ethanol (aq.) (*v/v*).
369
370 *3.6. Dynamic adsorption / desorption of amygdalin on D101 resin*
371
372 The dynamic adsorption/desorption experiment was performed by the column
373 chromatography with the D101 resin. The character of Langmuir type isotherm
374 implies that with the adsorption sites of adsorbent being covered, it is more and more
375 difficult for the adsorbate molecules to collide with adsorption sites, i.e., the adsorbate
376 molecules have no strong competition with the solvent molecules on the adsorbent
377 surface, and the adsorption finally reaches the equilibrium [24]. In order to evaluate
378 the relationship between the mass of resin and loading volume of TBK crude solutions,
379 the dynamic adsorption of amygdalin on D101 resin was investigated. According to
380 the definition of leakage point, results in Fig.3 (F) indicated that when the loading
381 volume was 64 ml, the concentration of amygdalin in effluent solution was 19.21 mg
382 l^{-1}, about 10% of the initial amygdalin concentration (207.25 mg l^{-1}). Therefore, the
383 most suitable loading volume of TBKs crude solution was 64 ml (about 1 BV). In
384 addition, the adsorption efficiency at three loading flow rate (1, 2 and 3 BV/h) were
385 87.84, 91.00 and 86.24%, respectively, which indicated the loading flow rate to give
386 the highest adsorption efficiency was 2 BV/h.

According to the above adsorption parameters, 64 ml TBKs crude solution with its initial amygdalin concentration of 302.72 mg l^{-1} was loaded onto a D101 resin packed glass column, and then washed by 3 BV distilled water to remove the non-adsorbed impurities such as proteins, polysaccharides, etc. The dynamic desorption curve of amygdalin eluted by ethanol (aq.) (40:60, *v/v*) was then obtained. As described in Fig.3 (G), about 650 ml (equivalent to 11 BV) of ethanol eluted the majority of the adsorbed amygdalin. The purity of amygdalin in the lyophilized eluent, as measured by HPLC (Fig. 4), was 82.0%, and the recovery of the amygdalin was 77.9%.

4. Conclusions

This study developed a method for separation and purification of amygdalin from TBKs. As a result of 82.0% purity and 77.9% recovery of amygdalin in the enriched product, D101 macroporous resin chromatography with the elution by 40% ethanol (aq.) (*v/v*) at 30°C was found suitable for the separation of amygdalin from the crude extracts with 4.8% purity. The results evidenced a good adsorption and separation potential of the D101 resin to amygdalin.

Conflict of interest

The authors declare that there are no conflicts of interest.

Acknowledgements

This research project was financially supported by the Program for Zhejiang Leading Team of Sci. & Technol. Innovation (2010R50032).

References:

[1] K.S. Chen, C.J. Xu, B. Zhang, I.B. Ferguson, Hortic. Rev. 30 (2004) 83.

[2] J. Cheng, X. Ye, J. Chen, D. Liu, S. Zhou, Food Chem. 107 (2008) 1674.

[3] Y. Zhang, S. Li, C. Yin, D. Jiang, F. Yan, T. Xu, Food Chem. 135 (2012) 304.

[4] J.Y. Koo, E.Y. Hwang, S. Cho, J.H. Lee, Y.M. Lee, S.P. Hong, J. Chromatogr. B 814 (2005) 69.

[5] J. Mu, J. Chin. Med. Mat. 25 (2002) 366.

[6] C. Zhou, L. Qian, H. Ma, X. Yu, Y. Zhang, W. Qu, X .Zhang, W. Xia, Carbohydr. Polym. 90 (2012) 516.

[7] J.Vetter. Toxicon, 38 (2000) 11.

[8] J. Deng, C. Li, H. Wang, E. Hao, Z. Du, C. Bao, J. Lv, Y. Wang, Biochem. Biophys. Res. Commun. 411 (2011) 523.

[9] H. Hwang, P. Kim, C. Kim, H. Lee, I. Shim, C. Yin, Y. Yang, D. Hahm, Biol. Pharm. Bull. 31 (2008) 1559.

[10] H. Hwang, H. Lee, C. Kim, I. Shim, D. Hahm, J. Microbiol. Biotechnol. 18 (2008) 1641.

[11] G.A. Fernandez, A.C. Lagunas, S.A. Llebaria, J.J. Perez, Europe Patent EP 1847270 B1 (2010).

[12] F. Nabavizadeh, A.M. Alizadeh, Z. Sadroleslami, S. Adeli, J. Med. Plants Res. 5 (2011) 3122.

[13] J. Li, H.A. Chase, Nat. Prod. Rep. 27 (2010) 1493.

[14] Y.J. Fu, Y.G.. Zu, W. Liu, C.L. Hou, L.Y. Chen, S.M. Li, X.G. Shi, M.H. Tong, J. Chromatogr. A 2(2007) 206.

[15] Q.P. Xiong, Q.H. Zhang, D.Y. Zhang, Y.Y. Shi, C.X. Jiang, X.J. Shi, Food Chem. 145 (2014) 1.

[16] F. Lalaguna, J. Chromatogr. A 657 (1993) 445.

[17] C. Datta, A. Dutta, D. Dutta, S. Chaudhuri, Procedia Food Sci. 1(2011) 893.

[18] A. Bunea, D. Rugină, Z. Sconţa, R. M. Pop, A. Pintea, C. Socaciu, J. VanCamp, Phytochem. 95 (2013) 436.

[19] A. A. García, B. C. Grande, J. S. Gándara, J Chromatogr. A. 1054 (2004) 175.

[20]W. Liu, S. Zhang, Y. Zu, Y. Fu, W. Ma, D. Zhang, Y. Kong, X. Li, Bioresour. Technol., 101 (2010) 4667.

[21] Y. Sun, H. Yuan, L. Hao, C. Min, J. Cai, J. Liu, P. Cai, S. Yang, Food Chem. 141 (2013) 533.

[22] National Pharmacopoeia Committee, Pharmacopoeia of the People's Republic of China (Part 1), Chemical Industry Press, Beijing, China (2010) pp.260

[23] Y.S. Ho, G. McKay, Chem. Eng. J. 70 (1998) 115.

[24] K. Seiichi, T. Ishikawa, I. Abe, Adsorption Science, Chemical Industry Press,

453 Beijing, China (2007) pp.119.
454 [25] I. Langmuir, J. Amer. Chem. Soc. 40 (1918) 1361.
455 [26] H. Freundlich, Z. Phys. Chem. 57 (1907) 385.
456 [27] J. Li, H.A. Chase, J. Chromatogr. A 1216 (2009) 8759.
457 [28] C. Nobrea, M.J. Santos, A. Dominguez, D. Torresa, O. Rocha, A.M. Peres, I.
458 Rocha, E.C. Ferreira, J.A. Teixeira, L.R. Rodrigues, Anal. Chim. Acta 654 (2009)
459 71.
460 [29] R. Wang, X. Peng, L. Wang, B. Tan, Y. Liu, Y. Feng, J. Sep. Sci., 35 (2012).1985.
461 [30] L. Lin, H. Zhao, Y. Dong, B. Yang, M. Zhao, Food Chem.130 (2012) 417.
462 [31] G. Annadurai, S. Rajesh, K.P.O. Babu, T. Mahesh, T. Murugesan, Bioprocess
463 Biosys. Eng. 22 (2000) 493.
464 [32] P.R. Brown, E. Grushka, Adv. Chromatogr. 42 (2001) 25.
465

466 Fig.1 Chemical structure of amygdalin

467 Fig.2 HPLC chromatograms of authentic amygdalin standard (A) and crude TBK
468 sample (B)

469 Fig.3 Adsorption/desorption behaviors of amygdalin from TBKs extract on MARs. (A)
470 Adsorption/desorption ratios of amygdalin on different resins (the number in X-axis
471 represented different types of resins: 1.HPD722, 2.HPD720, 3.AB-8, 4.NKA-9,
472 5.D101, 6.HPD100, and 7.HPD400). Different lowercase letters above each bar
473 represented significance difference at $P<0.05$. Experiments were done in triplicate; (B)
474 Adsorption capacity and desorption ratio of amygdalin on three types of resins and
475 three amygdalin concentrations at 30 °C; (C) Static adsorption kinetics of amygdalin
476 on D101 resin; (D) Adsorption isotherm of amygdalin on D101 resin at 30 °C. Point A
477 was the equilibrium concentration (C_e) of amygdalin solution corresponding to the
478 adsorption capacity when the initial concentration was 129.13 mg/L, and Point B was
479 that of 358.68 mg/L; (E) Effect of ethanol concentration on desorption ratio of
480 amygdalin on D101 resin. Different lowercase letters above each bar represented
481 significance difference at $P<0.05$. Experiments were done in triplicate; (F) Dynamic
482 adsorption curve of amygdalin on D101 resin; and (G) Dynamic desorption curve of
483 amygdalin on D101 resin.

484 Fig.4 The chromatogram of enriched amygdalin after D101 resin purification

485 Fig.1 *T. Wang, et al.*

486

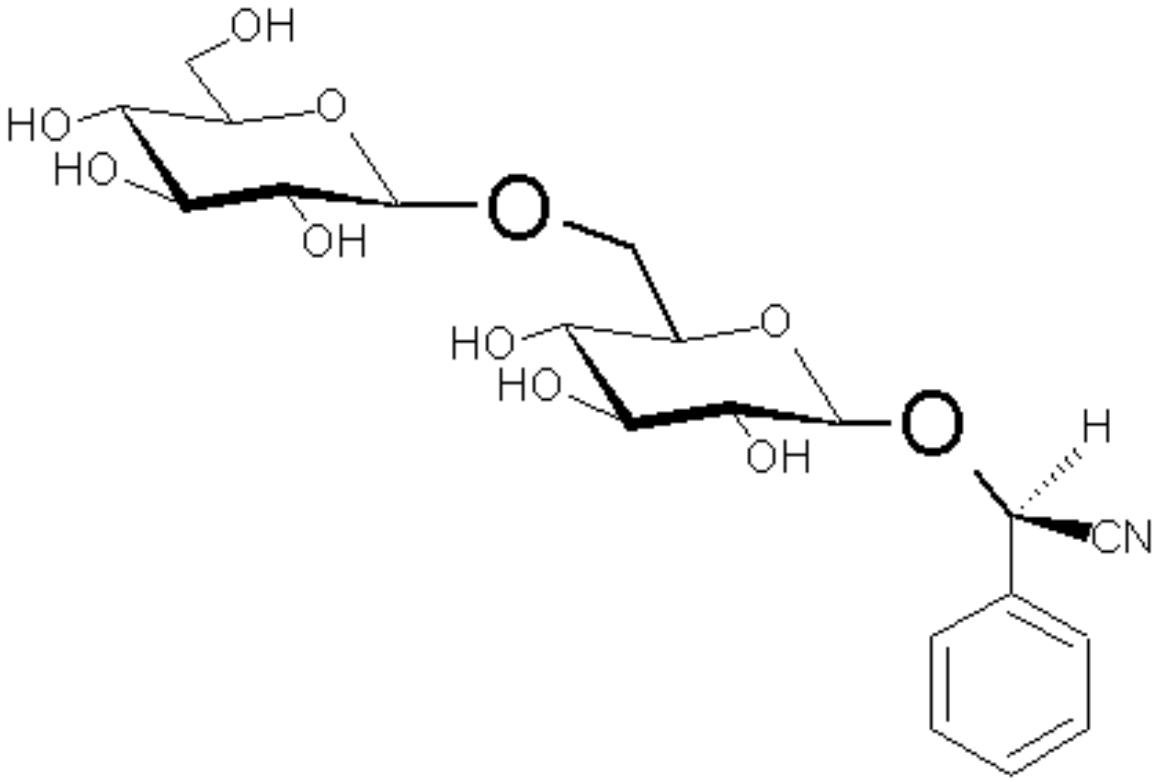

487

488

489 Fig.2 (A) and (B) *T. Wang, et al.*

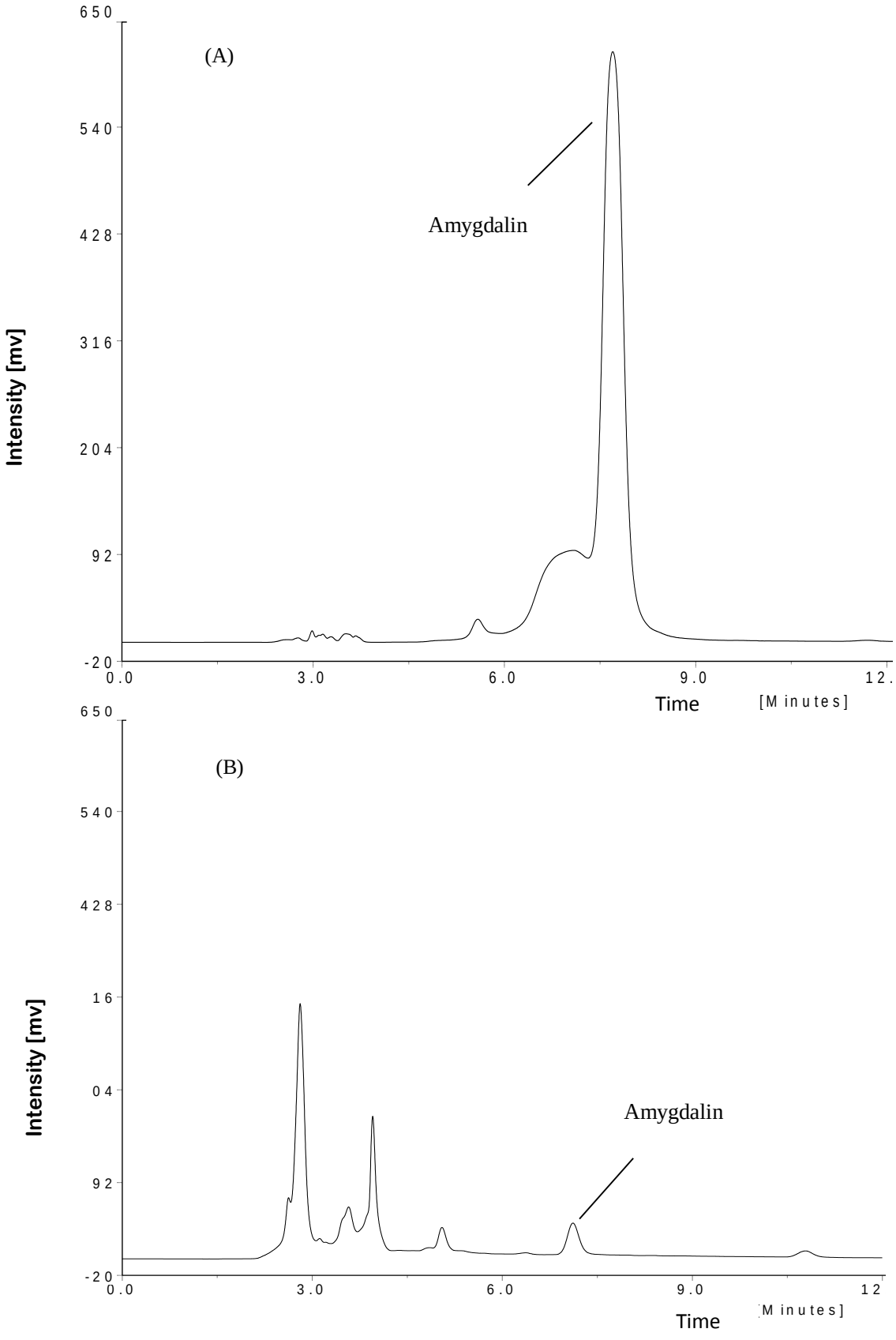

490

491 Fig.3 (A)- (G) *T. Wang, et al.*

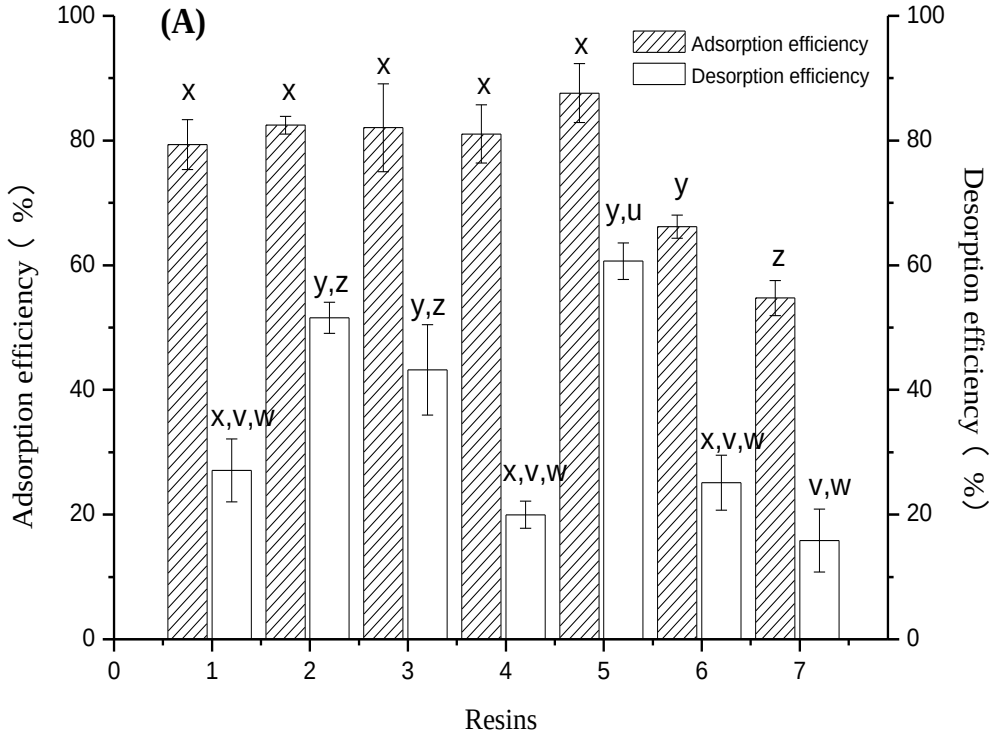

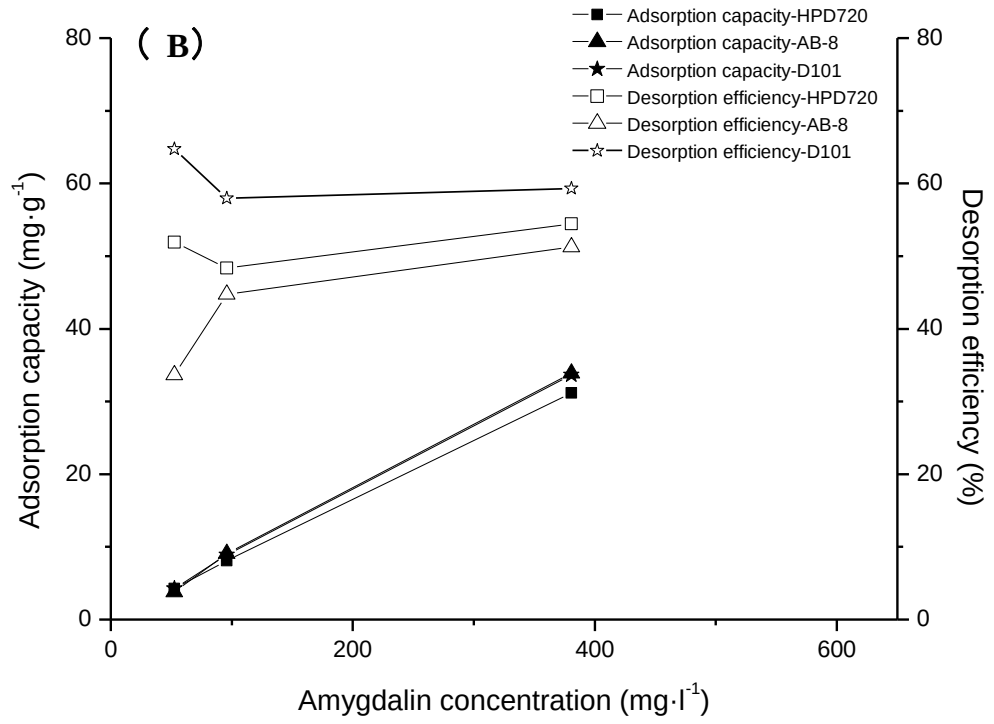

492

493

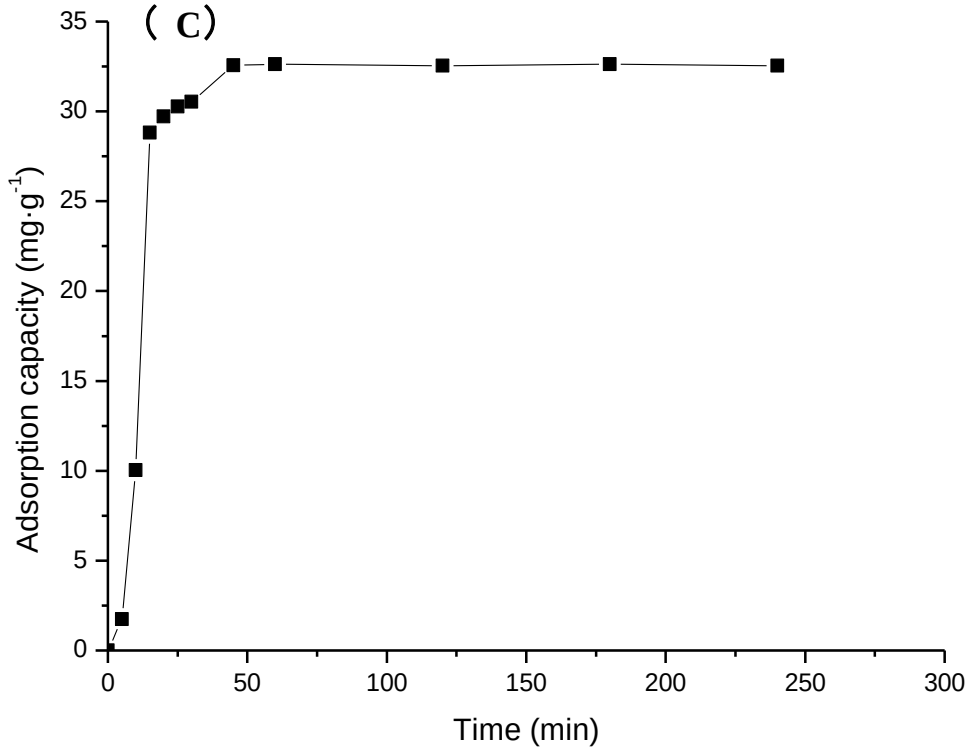
(C)
Adsorption capacity (mg·g-1)
Time (min)
0
5
10
15
20
25
30
35
0
50
100
150
200
250
300

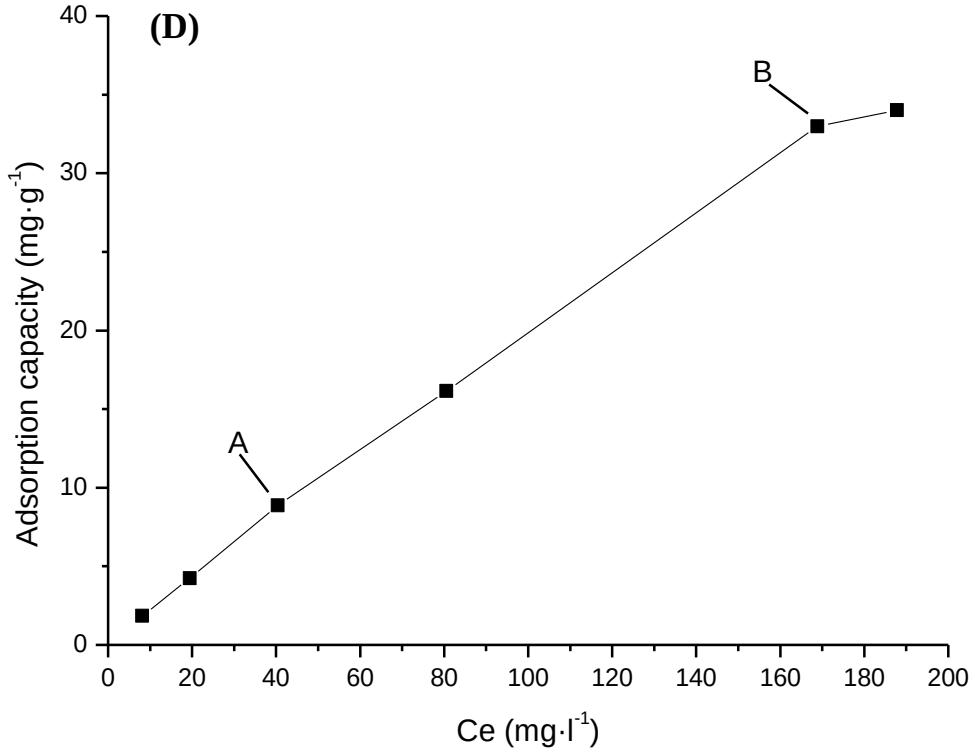
(D)
Adsorption capacity (mg·g-1)
Ce (mg·l-1)
A
B
0
10
20
30
40
0
20
40
60
80
100
120
140
160
180
200

495

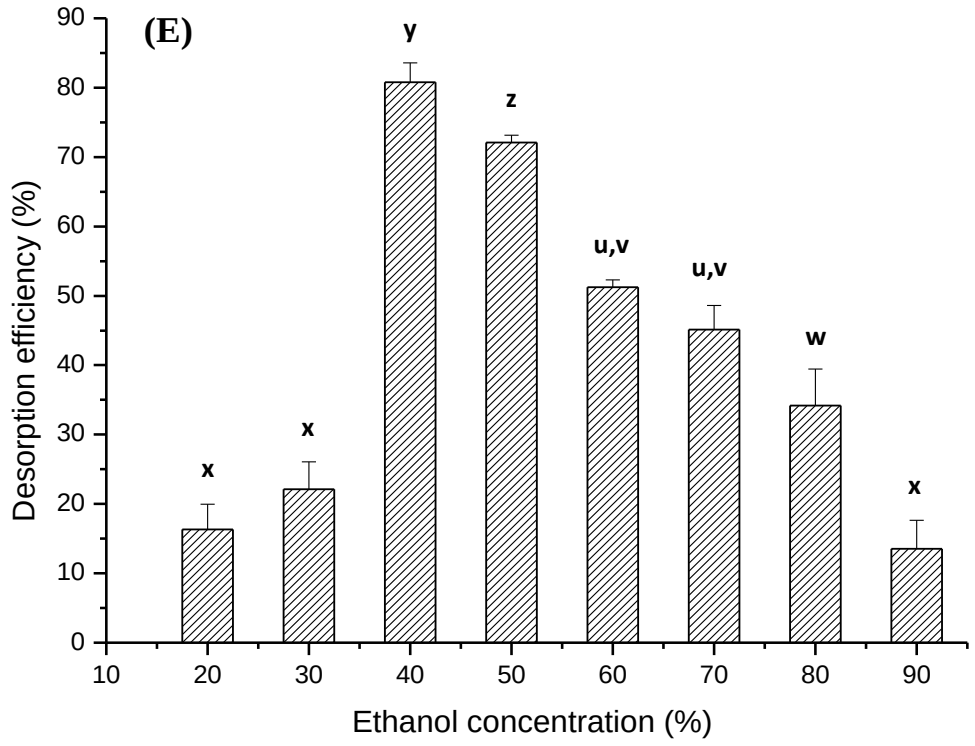
(E)
Desorption efficiency (%)
Ethanol concentration (%)
x
x
y
z
u,v
u,v
w
x

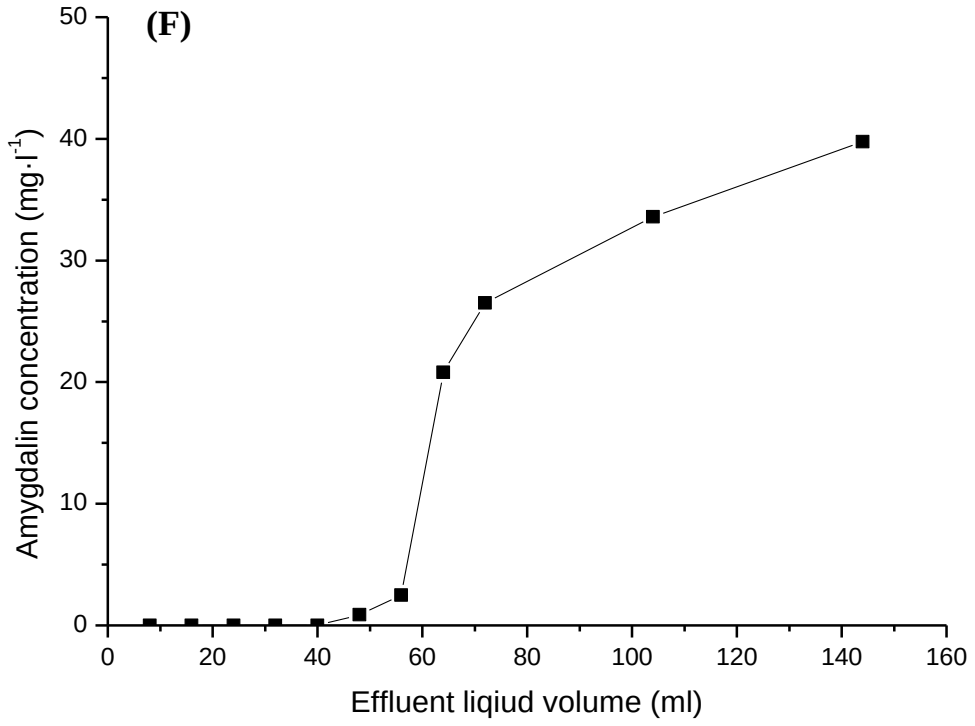
(F)
Amygdalin concentration (mg·l-1)
Effluent liqiud volume (ml)

497

498 Fig.3 (A)- (G) *T. Wang, et al.*

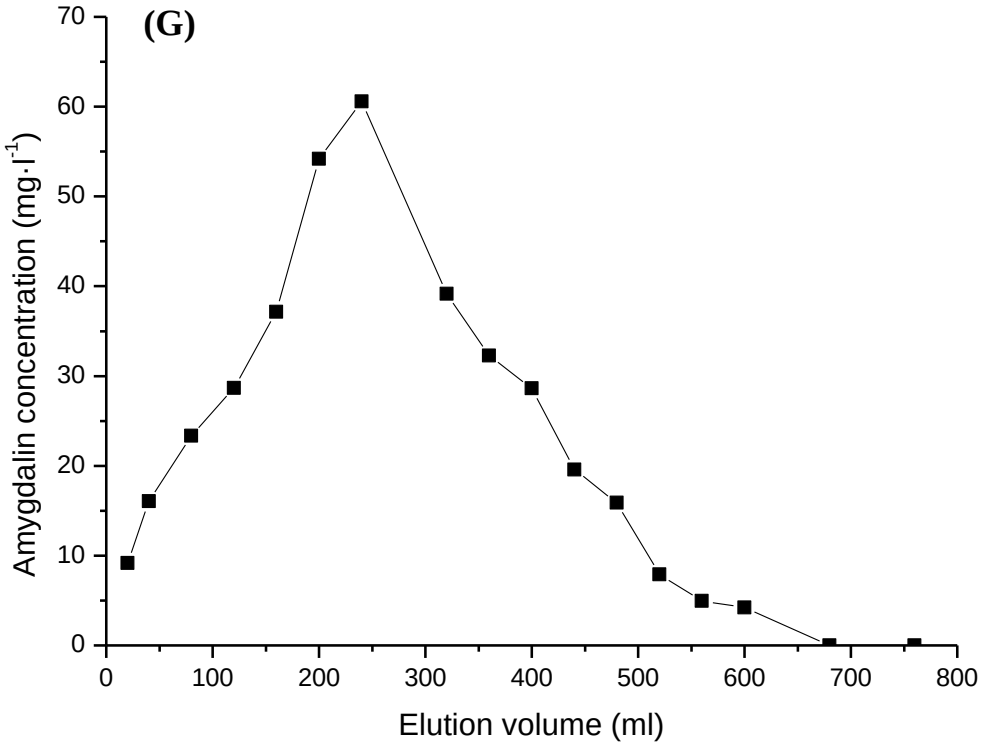

499

500 Fig.4 *T. Wang, et al.*

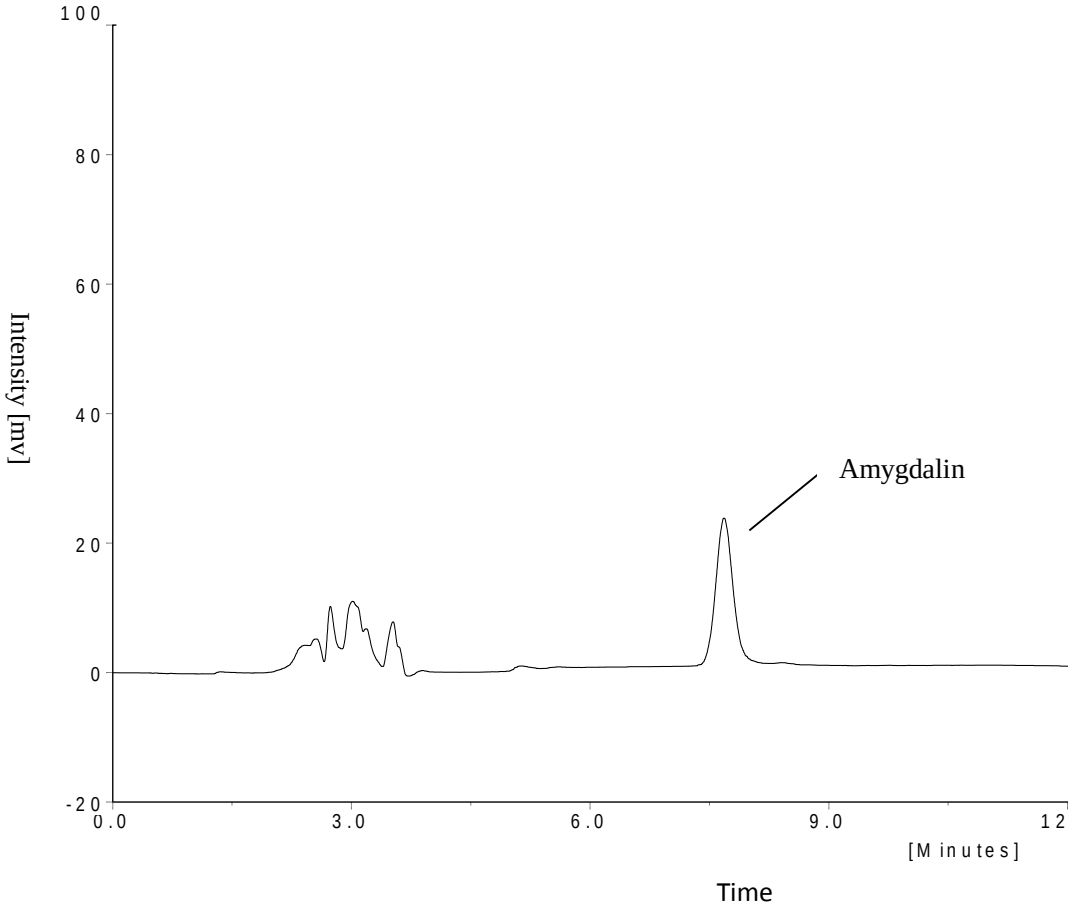

501
502

503 Table 1 Physical properties and the moisture contents of the macroporous adsorption

504 resins

Resin	Polarity	Structure	Specific surface area (m^2 g^{-1})	Pore size (nm)	Moisture content (%)
HPD722	Weak	SDVB	485-530	13.0-14.0	69.91
HPD720	Weak	SDVB	-	-	67.52
AB-8	Weak	SDVB	≥480	13.0-14.0	71.07
NKA-9	Weak	SDVB	250-290	15.5-16.5	72.76
D101	Non	SDVB	≥550	9.0-10.0	70.66
HPD100	Non	SDVB	650-700	8.5-9.0	51.45
HPD400	Medium	SDVB	500-550	7.5-8.0	68.69

505 "-" : not specified. SDVB: styrene divinyl-benzene.

506

507 Table 2 Langmuir and Freundlich parameters of amygdalin on D101 resin at 30 °C

Langmuir	
Linear equation	$C_e/q_e = 4.4313 + 0.0052C_e$
R^2	0.9060
q_0 (mg/g)	192.3077
K_L	0.0012
Freundlich	
Linear equation	$q_e = 0.3080C_e^{0.9040}$
R^2	0.9974
K_F	0.3080
n	1.1062

508